

Imaging the complex geology of the Faroe Shetland Basin, West of Shetlands

Matthew Hart, Guy Hilburn, Sandeep Bhamber, Jason Twigg, Rachel Ward, Steve Drewell & Simon Baldock
TGS

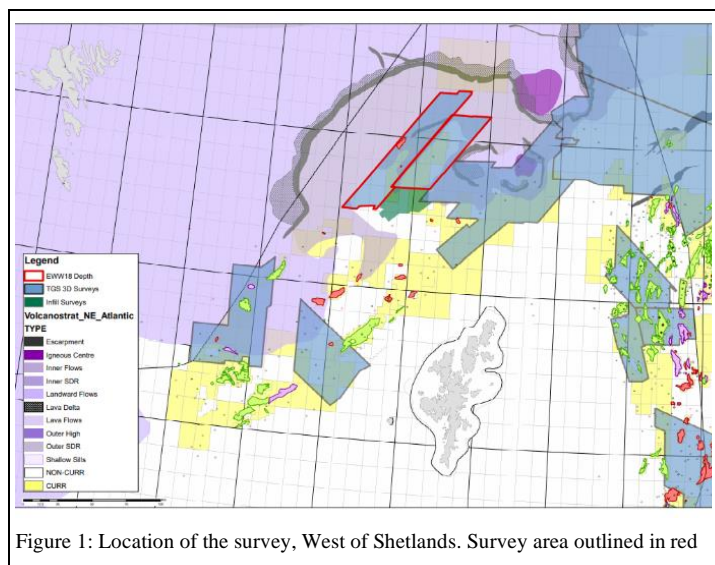


Figure 1: Location of the survey, West of Shetlands. Survey area outlined in red

Summary

The Faroe Shetland Basin area located to the West of the Shetland Islands is typified by complex structural features with highly variable velocities, often with sharp contrasts.

We present an imaging workflow, incorporating an efficient high-resolution velocity model building method, to optimally image these structures, particularly focusing on Eocene sand fans and injectites. This was achieved with a combination of careful pre-processing to preserve diffraction energy and complex moveout and velocity model building with image guided tomography and phase only reflection FWI. By incorporating image guided travel time tomography constraints alongside the reflection FWI, we were able to update the background trend as well as the fine details and velocity contrasts of these features simultaneously. By doing so, we reduce the need for additional migrations and improve project turnaround.

Introduction

During 2018, 1900 km² of narrow-azimuth 3D streamer data were acquired in the northeast of the Faroe Shetland Basin. Data were acquired using a triple-source, continuous recording configuration, with 12 x 8 km conventional hydrophone streamers towed at a nominal depth of 12 m. This was merged with earlier vintage acquisition from 1996,

1997, 1999 and 2012, to give a total area of 3900 km² (figure 1).

The Faroe Shetland Basin is notable for its complex geology, of particular note being Eocene sand fans, injectites, significant faulting and the complex volcanics present in the area, consisting of both intrusive sills and extrusive lava flows. These structural features can present significant velocity contrasts over small scales which can prove challenging to image using conventional velocity model building approaches.

Pre-processing

Deblending by sparse inversion

In order to increase trace density and enhance spatial resolution, data were acquired with a blended acquisition configuration with overlapping shot records. This also had the benefit of improving acquisition efficiency. However, energy from the preceding and subsequent shots is present in each shot record and must be removed.

To achieve this overlapping source separation we adopt an inversion based approach, following the methodology of Masoomzadeh et al. (2019), where iterative modelling of high amplitude and coherent events is achieved with iterative amplitude thresholding in the $f-kx-ky$ domain until the residual energy (the difference between the input and the reblended model shots) becomes insignificant.

Noise attenuation

Due to marginal weather conditions during acquisition, swell noise was significant in places. We adopted a statistical approach to identifying areas of particularly strong swell noise, by measuring the noise/signal ratio for each trace. This method was designed to be unbiased by deep high amplitude primary or multiple reflections. A higher ratio points to stronger swell noise in data prior to deghost. Targeted attenuation techniques could then be used to remove this.

Linear noise was not targeted pre-migration, to preserve diffraction tails and retain as much primary energy as possible during the migration.

Debubble using near-field hydrophones

Low-frequency energy, which is particularly important for imaging beneath volcanics and velocity model building with

Imaging the complex geology of the Faroe Shetland Basin, West of Shetlands

FWI, is recovered during the deghosting process. Unwanted bubble energy will also be boosted by this process, so it is important that this is attenuated beforehand. This is achieved using near-field hydrophone (NFH) recordings to derive shot-by-shot debubble operators. These operators can also compensate for source variations during acquisition.

To create a bubble-free target wavelet, NFH recordings are converted to far field signatures via an inversion of the near-field hydrophone recordings (Ziolkowski et al., 1982; Parkes et al., 1984).

NFH information was not utilized for vintage acquisition, instead a source signature was derived from the data to remove bubble energy.

Inversion deghosting

Source and receiver ghosts were removed from the data separately. Receiver deghosting was performed using inversion-based deghosting in the 3D tau- px - py domain Zhang et al., (2018). This method requires that the receiver depths are known. As we expect some variability in the streamer depth and sea surface, we perform a search based on a minimum energy criterion in the f - x domain to accurately determine receiver depths (Hardwick et al., 2015). Source-side deghosting is performed separately using a 2-D approximation in the f - k domain.

Demultiple

In order to protect primary diffracted energy and complex moveout, pre-migration multiple attenuation was handled exclusively by 3D SRME. Radon demultiple was used post-migration to attenuate residual multiple energy after diffractions had been collapsed and complex moveout resolved with high-resolution velocity model building and TTI Kirchhoff pre-stack depth migration.

Survey merge

Amplitude and timing of the legacy data were matched to the new acquisition, to create a homogenous dataset across vintages. Data were then regularised onto the 12.5 m by 12.5 m migration grid using 4D Anti-leakage Fourier Transform regularisation.

Velocity Model Building

Initial Model

During pre-processing, velocity picking was carried out to generate a 2 km by 2 km velocity model. A heavily smoothed version of this model was used as a starting point for depth velocity model building, so as not to influence the outcome

and bias the result with any pre-existing detail contained within the model.

Water velocity in the West of Shetlands region is known to be extremely variable. To minimise the effect of this on the migrated image, temperature and salinity information (TS dip) were utilised to calculate water velocity throughout the survey area / time of acquisition. As expected, this was seen to vary spatially due to time of acquisition by as much as 5 m/s between acquisition sequences, over the first 500 m of the water column. A series of scans were used to evaluate moveout at the water bottom and scale the water column model accordingly. An accurate water velocity is a key starting point for velocity model building, otherwise inaccuracies may be extended into the sedimentary velocity model. An inaccurate water velocity model would also cause mismatches for FWI and skew the resulting model to compensate, which may lead to cycle-skipping in the data.

Anisotropy was calculated at the Bunnehaven well location after calibration and was structurally extrapolated out across the survey area. Due to the limited well control available, this model was simplified to a Gaussian function, which was thought to best represent the compression gradient expected in the shallow sediments.

Image Guided Tomography

The first stages of model building concentrated on updating the sediments between water bottom (~1500 m) and the Balder formation (~3400 m). Initial updates were focussed on correcting the background velocity trend. Subsequent passes incorporated image guided tomography (Hilburn et al., 2014), including offset dependent moveout picking and image guided inversion constraints increasing the complexity of the resulting velocity update.

This initial stage of model building was seen to flatten gather moveout down to Balder, indicating background velocity was appropriate to begin a more detailed Full Waveform Inversion model update.

Reflection FWI

The water column in the survey area is quite deep, ranging between 1.1 and 1.8 km. In addition to this, the vintage data were acquired in 2012 with a 6 km streamer. This combination of deep water and available offset from the streamer acquisition meant that diving wave energy was limited or entirely absent throughout the survey area. The maximum depth of a diving wave FWI update was calculated as approximately 200 m below water bottom for the 2018 acquisition with 8 km streamers. As such, a conventional diving wave approach was not deemed suitable for this data.

Imaging the complex geology of the Faroe Shetland Basin, West of Shetlands

Reflection FWI was required in order to build a detailed model of the complex and variable geology of the area, incorporating sand injectites, Eocene fans and polygonal faulting seen in the shallow sediments. For this we use a phase-only approach, which utilizes a local-correlation based objective function after dynamically matching the two datasets. This approach is described in more detail by Sheng (2020).

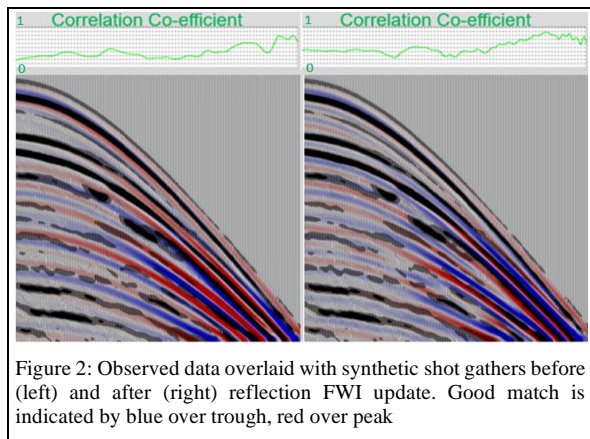


Figure 2: Observed data overlaid with synthetic shot gathers before (left) and after (right) reflection FWI update. Good match is indicated by blue over trough, red over peak

Reflection FWI was then used to invert the injectites, Eocene fan features and faulting present in the sediments above Balder. Several iterations were carried out through increasing frequency bands, starting at 5 Hz due to lack of low frequency signal in the vintage acquisition, up to a maximum frequency of 10 Hz. These updates were verified by reviewing the correlation cost function and data fit on shot gathers. An example of the data fit before and after update can be seen in figure 2, showing a better match between observed and synthetic gathers and improved correlation after FWI

During the FWI run, constraints were applied in both data and model domains to improve the convergence. In the model domain, a low-resolution tomographic constraint was incorporated in order to stabilise the background velocity and optimally flatten the gathers, whilst retaining the high-resolution features.

To validate this approach, comparisons were made with a more conventional iterative workflow consisting of reflection FWI followed by tomography. Gather response, spatial distribution and histograms of residual moveout (gamma) were used to evaluate the results. As can be seen in the gamma histograms (figure 3), results were statistically identical with the different approaches.

This approach also preserves the high-resolution details modelled by reflection FWI, as the constraint is only

updating the background model. Examples of the details captured by this modelling approach can be seen in figure 4 showing the shallow injectites (inset).

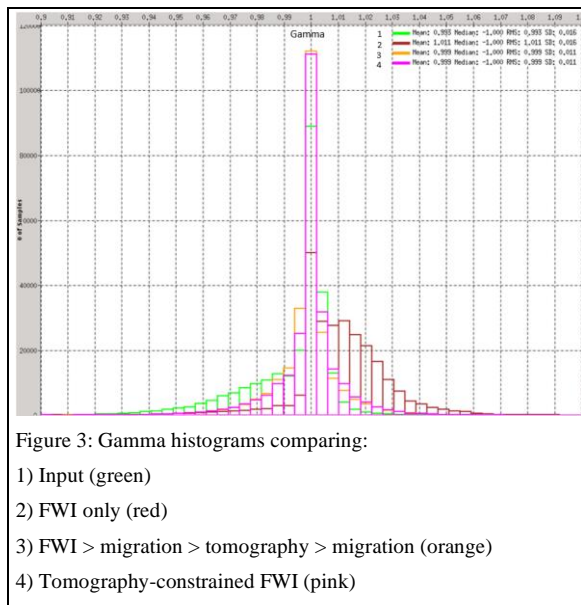


Figure 3: Gamma histograms comparing:
1) Input (green)
2) FWI only (red)
3) FWI > migration > tomography > migration (orange)
4) Tomography-constrained FWI (pink)

Further passes of image-guided tomography were subsequently run to update beneath the Balder horizon and Flett unconformity. This package consisted largely of high contrast volcanics and lower velocity sedimentary layers. With this image guided approach, it was possible to build a detailed model of these volcanic features, including sills, extrusives and the inner flows, also shown in figure 4.

Results

With careful processing of data prior to migration we were able to retain all diffraction energy and complex moveout whilst still optimally eliminating noise and multiple. Deghosting enhanced the resolution of the data, resulting in improved imaging of key geological features.

Fault planes and structures are preserved and better positioned, whilst the resulting image is improved beneath complex events, as can be seen in figure 5. The Balder and Flett horizons in the original processing appeared undulating and broken up, due to inaccuracies in the overburden model. With a more detailed model these layers are now significantly better imaged, which also has positive implications for the less conformable layers beneath.

Imaging the complex geology of the Faroe Shetland Basin, West of Shetlands

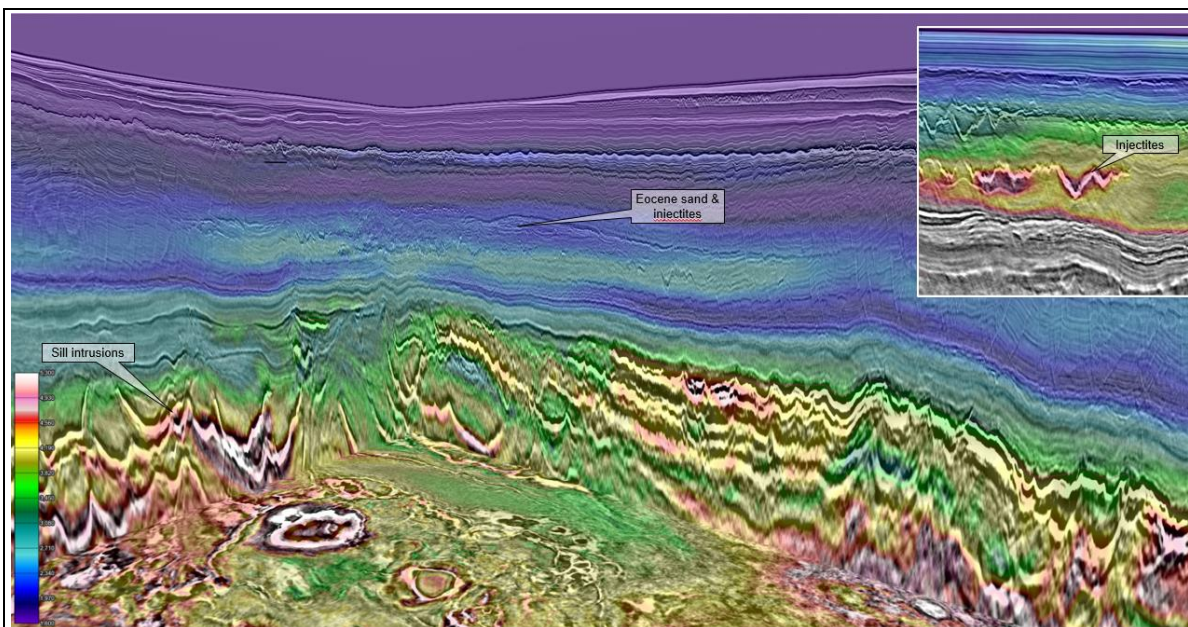


Figure 4: Final velocity model, highlighting main structural features in the region

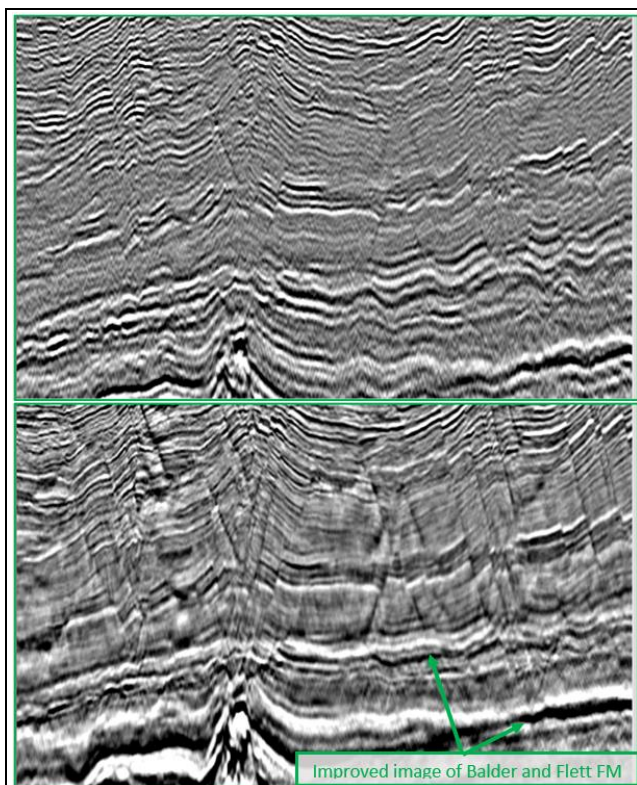


Figure 5: Vintage processing (top) vs. reprocessing (bottom)

Conclusions

By incorporating image guided travelttime tomography and FWI, we have been able to produce a detailed velocity model of the complex geology of the Faroe Shetland Basin region. It has also been possible to update both background velocity trends and higher resolution velocity variations simultaneously using a tomography constraint in the reflection FWI workflow and in doing so, reduce the need for additional migrations and improve project turnaround. This, in conjunction with careful pre-processing produced a significant uplift over the original vintage processing.

Improvements to imaging of the volcanic events may be investigated with a reverse time migration in future work, utilising more detailed models of the volcanics and inter basalt sediments in the deep. The volcanic features represented in this area are analogous to those found throughout much of the Atlantic Margin region, so successful imaging through these events will prove key to future exploration in the region.

Acknowledgements

The authors would like to thank John Millet and Ben Manton from VBPR and Reidun Myklebust from TGS for their assistance in understanding the geology of the region, our colleagues who have worked on this data over the past year, our clients for their input throughout processing and TGS for permission to present our results.

REFERENCES

- Hardwick, A., P. Charron, H. Masoomzadeh, A. Aiyepuku, P. Cox, and A. Laha, 2015, Accounting for sea surface variation in deghosting — A novel approach applied to a 3D dataset offshore west Africa: 85th Annual International Meeting, SEG, Expanded Abstracts, 4615–4619, doi: <https://doi.org/10.1190/segam2015-5901526.1>.
- Hilburn, G., Y. He, Z. Yan, and F. Sherrill, 2014, High-resolution tomographic inversion with image-guided preconditioning and offset-dependent picking: 84th Annual International Meeting, SEG, Expanded Abstracts, 4768–4772, doi: <https://doi.org/10.1190/segam2014-1219.1>.
- Masoomzadeh, H., S. Baldock, Z. Liu, H. Roende, C. Mason, and H. Pal, 2019, Deblending of long-offset OBN data for velocity model building by sparse inversion of hyperboloidal components: 89th Annual International Meeting, SEG, Expanded Abstracts, 4053–4057, doi: <https://doi.org/10.1190/segam2019-3216531.1>.
- Parkes, G. E., A. Ziolkowski, L. Hatton, and T. Haugland, 1984, The signature of an air gun array: Computation from near field measurements including interactions — Practical considerations: *Geophysics*, **49**, 105–111, doi: <https://doi.org/10.1190/1.1441640>.
- Sheng, J., J. Mao, and F. Liu, 2020, A robust full waveform inversion of reflection data with data constraint: EAGE 2020 extended abstract submission.
- Zhang, Z., H. Masoomzadeh, and B. Wang, 2018, Evolution of deghosting process for single sensor streamer data from 2D to 3D: *Geophysical Prospecting*, **66**, no. 5, 975–986, doi: <https://doi.org/10.1111/1365-2478.12614>.
- Ziolkowski, A., G. Parkes, L. Hatton, and T. Haugland, 1982, The signature of an air gun array: Computation from near field measurements including interactions: *Geophysics*, **47**, 1413–1421, doi: <https://doi.org/10.1190/1.1441289>.